Journal of Colloid and Interface Science 333 (2009) 329–334

Contents lists available at ScienceDirect

Journal of Colloid and Interface Science

www.elsevier.com/locate/jcis

A simple approach to the synthesis of hollow microspheres with magnetite/silica hybrid walls

Jia Liu, Yonghui Deng *, Chong Liu, Zhenkun Sun, Dongyuan Zhao *

Department of Chemistry, Shanghai Key Laboratory of Molecular Catalysis and Innovative Materials, Advanced Materials Laboratory, Fudan University, Shanghai 200433, PR China

ARTICLE INFO

Article history:
Received 26 September 2008
Accepted 4 February 2009
Available online 11 February 2009

Keywords:
Synthesis
Templating
Hollow microspheres
Mesoporous materials
Magnetic
Sol–gel

ABSTRACT

In this paper, we report a simple approach for templating synthesis of magnetic hollow composite microspheres with magnetite/silica walls. This approach is based on the co-sedimentation of polymer microspheres and magnetic colloids followed by impregnation with silica oligomer from tetraethyl orthosilicate and the further removal of the polymer microspheres by pyrolysis. The diameter of the hollow microspheres can be adjusted in range of 300 nm–2.0 μm by using polymer microspheres of different sizes and the wall thickness is tunable from 10–50 nm by controlling ratio of magnetite to the polymer microspheres. Magnetic characterizations show that the hollow microspheres have superparamagnetism with magnetization saturation of 10–30 emu/g. HRTEM and N_2 adsorption–desorption isotherms reveal that the hollow microspheres have numerous nanopores in the walls with a broad distribution in the range of 2 to 80 nm, which results in a high BET surface (67.6 m^2/g) and pores volume (0.14 cm^3/g).

1. Introduction

In the past decade, hollow microspheres [1–4] have attracted much attention for their potential applications in various fields including drug-delivery carriers [5–7], efficient catalysts [8–11], imaging [12,13], nanoscale reactors [14,15], photonic crystals [16,17] and so on [18–21]. A variety of hollow microspheres with diverse sizes and wall compositions have been reported. The most frequently used method for the preparation of hollow microspheres is a templating approach, which relies on the use of various removable templates such as silica microspheres [22,23], polymer latexes [3,7], emulsion droplets [5,16], and even gas bubbles [12]. It has been demonstrated that the layer-by-layer (LbL) assembly [3] based on silica or polymer microspheres as sacrificial templates is a versatile and reproducible technique, which results in a large number of hollow microspheres or microcapsules. The template-free approach which can simplify the preparation procedure has been developed recently. This approach often involves some unusual mechanisms including differential diffusion (Kirkendall effect) within metastable solid microspheres [18,24], corrosion-based inside-out evacuation [13] and inside-out Ostwald ripening [25].

More recently, functional hollow microspheres have aroused increasing interest not only for their large inner void, low density and high surface area, but also because of the useful properties such as optics, electrics, magnetism, thermoresponsivity, pH sensitivity [26–30]. For example, through the LbL approach by alternating adsorption of oppositely charged polyelectrolytes (PE) on colloidal microsphere cores followed by core dissolution and further modification with silver nanoparticles, Radziuk et al. [31] synthesized hollow PE microspheres with surface modified by silver nanoparticles and achieved a remote opening of the PE/Ag microspheres with a laser. The rupture time for the PE/Ag microspheres could be adjusted from 7 to 26 s by using silver nanoparticles with different sizes. Due to unique magnetic responsivity, magnetic hollow microspheres are favorable for convenient manipulation in practical applications such as separation and enrichment, magnetically guided drug delivery. Caruso and coworkers [32,33] successfully synthesized magnetic hollow microspheres through a multistep LbL strategy by coating positively charged multilayered PE-coated polystyrene latexes with magnetite nanoparticles, followed by calcination to remove the polystyrene templates. However, it suffers from time-consuming and tedious synthetic procedures including repeated washing PE after each adsorption, and therefore it is not suitable for large-scale synthesis. Qiao et al. [34] reported the fabrication of magnetic cobalt hollow microspheres in one-step solvothermal reaction. Unfortunately, the toxicity and the lack of functional surface of the cobalt hollow microspheres greatly limit their applications, especially in biomedical domain.

* Corresponding authors. Fax: +86 21 6564 1740.
E-mail addresses: yhdeng@fudan.edu.cn (Y. Deng), dyzhao@fudan.edu.cn (D. Zhao).

0021-9797/$ – see front matter
doi:10.1016/j.jcis.2009.02.013

Herein, we report a simple approach for templating synthesis of magnetic hollow microspheres with magnetite/silica composite walls through the co-sedimentation of polymer microspheres and magnetic colloids followed by cross-linking of silicate oligomers from tetraethyl orthosilicate (TEOS). After calcination to remove polymer microspheres, the obtained hollow microspheres have uniform diameter in the range of 300–2.0 μm adjusted by using different size polymer microspheres. The wall thickness is tunable from 10–50 nm by controlling ratio of magnetite to the polymer microspheres. Magnetic characterizations show that the hollow microspheres have superparamagnetism with high magnetization saturation of 10–30 emu/g. N_2 adsorption–desorption isotherms show that the hollow microspheres have numerous nanopores in the walls with a broad distribution in the range of 2 to 80 nm, which results in a relatively high BET surface (67.6 m^2/g) and pores volume (0.14 cm^3/g).

2. Materials and methods

2.1. Chemicals

3-(Trimethoxysilyl) propyl methacrylate (TMSPM) and polyvinylpyrrolidone (PVP, $M_w = 30000$) were purchased from Aldrich and used as received. 2,2-Azobisisobutyronitrile (AIBN) from Acros was re-crystallized in methanol before use. Styrene (St), $FeCl_2 \cdot 4H_2O$, sodium nitrite, concentrated HCl, trisodium citrate, tetraethyl orthosilicate (TEOS) and ethanol were purchased from Shanghai Chem. Corp. The polymerization inhibitor was removed from the styrene by infiltration through Al_2O_3 column. Distilled water was used in this study.

2.2. Synthesis

2.2.1. Synthesis of polymer microspheres

The polystyrene-*co*-poly-3-(trimethoxysilyl)propyl methacrylate (St-*co*-TMSPM) microspheres with a mean size of 500 nm were prepared through a dispersion polymerization approach [35]. For a typical preparation, 10 g of styrene, 8.0 g of polyvinylpyrrolidone, 2.5 g of 3-(trimethoxysilyl)propyl methacrylate and 0.20 g of 2,2-azobisiso-butyronitrile (AIBN) were dissolved in a mixture of ethanol (140 mL) and H_2O (10 mL). The obtained solution was then added into a 250 mL four-neck round bottom flask equipped with a mechanical stirrer, a refluxing condenser, and a nitrogen inlet. After sealing in a nitrogen atmosphere, the reactor was submerged in a water bath and the polymerization was carried out with a stirring speed of 100 rpm at 70 °C for 24 h. The resulting polymer microspheres were repeatedly washed with an ethanol–water mixture (1:1 volume ratio) by centrifugation and then dried at 30 °C. Finally, the microspheres were re-dispersed in water to obtain a colloidal solution (2 wt%) for further use.

2.2.2. Synthesis of magnetic fluid

Magnetite nanoparticles were synthesized through a simple redox reaction in a dilute aqueous solution. 0.80 g of sodium nitrite was firstly dissolved in an aqueous solution (1000 mL) containing 5.2 g of $FeCl_2 \cdot 4H_2O$, 100 mL of HCl (2.0 M). After stirring for about 5 min, 50 mL of concentrated aqua ammonia was added to the solution with stirring. The resulting solution was rapidly stirred for 30 min, and the black precipitate was separated with a magnet. In order to produce well dispersed magnetic dispersion, the obtained magnetite was ultrasonicated in nitric acid aqueous solution (100 mL, 2.0 M) for 2 min and subsequently separated from the solution and re-dispersed in a sodium citrate aqueous solution (100 mL, 0.5 M) with ultrasonic vibration. This treatment could introduce citrate groups on the magnetite nanoparticles, and thus enhancing their hydrophilicity and dispersibility [36]. Finally, the magnetite nanoparticles were collected and re-dispersed in water to obtain a stable magnetic fluid with a solid content of 0.4 wt% for further use.

2.3. Fabrication of magnetic hollow silica microspheres

25 g of magnetic fluid and 5.0 g of polymer microspheres colloidal solution were mixed by ultrasonication vibration. The obtained dispersion was evaporated in a glass vial at 40 °C for 48 h for the co-sedimentation of polymer microspheres and magnetite nanoparticles. After further drying in vacuum, the obtained polymer/Fe_3O_4 composite flakes were immersed in a silica sol solution for 3 times. The silica sol solution was prepared in advance by mixing tetraethyl orthosilicate (0.90 g), H_2O (2.0 mL), ethanol (10 mL) and hydrochloric acid (2.0 M, 0.10 mL) for 1 h. After completely dried, the composite was calcined in N_2 at 400 °C for 5 h with a heating rate of 2 °C/min before reaching 400 °C.

2.4. Characterization methods

Scanning electronic microscopy (SEM) images were recorded on a Philips XL30 electron microscope (Netherlands) operating at 20 kV. A thin gold film was sprayed on the sample before measurements. Transmission electron microscopy (TEM) images were taken with a JEOL 2011 microscope (Japan) operated at 200 kV. Samples were first dispersed in ethanol and then collected using carbon-film-covered copper grids for analysis. FT-IR spectra were collected on Nicolet Fourier spectrophotometer using KBr pellets (USA). Powder X-ray diffraction (XRD) patterns were recorded on a Bruker D4 X-ray diffractometer with Ni-filtered CuK_R radiation (40 kV, 40 mA). Thermogravimetric analysis (TGA) was carried out using a Mettler Toledo TGA-SDTA851 analyzer (Switzerland) from 25 to 800 °C under N_2 with a heating rate of 5 °C/min. Nitrogen sorption isotherms were measured on a Micromeritics Tristars 3000 analyzer at −196 °C. Before the measurements, the samples were degassed at 160 °C in a vacuum for 6 h. The Brunauer–Emmett–Teller (BET) method was utilized to calculate the specific surface areas. The pore size distributions were derived from the adsorption branches of the isotherms using the Barrett–Joyner–Halenda (BJH) method. The total pore volumes were estimated from the amount adsorbed at a relative pressure of $P/P_0 = 0.98$.

3. Results and discussion

The fabrication procedure mainly involves three steps as illustrated in Scheme 1. Firstly, poly(styrene-*co*-3-(trimethoxysilyl) propyl methacrylate) (Poly(St-*co*-TMSPM)) microspheres and magnetic fluid were dispersed in water by ultrasonication to form a stable dispersion, and the dispersion was placed in an oven at 40 °C for 48 h for the evaporation of water and co-sedimentation of Poly(St-*co*-TMSPM) microspheres and magnetite nanoparticle. After drying in vacuum, thin polymer microspheres/Fe_3O_4 composite flakes were obtained. Secondly, the flakes were impregnated with silicate sols by immersion of a pre-hydrolyzed TEOS in ethanol containing small amount of aqueous HCl solution. Thirdly, the silica impregnated flakes were dried naturally and pyrolyzed in N_2 atmosphere to remove the polymer microsphere templates, and after subsequent ultrasonication treatment in aqueous solution, dispersed magnetic hollow microspheres were obtained.

Poly(St-*co*-TMSPM) microspheres were synthesized through dispersion polymerization using poly(vinylpyrrolidone) (PVP) as a steric stabilizer according to the previous report [35]. The size of the microspheres can be tuned from hundreds of nanometer to several micrometers by varying the concentration of the

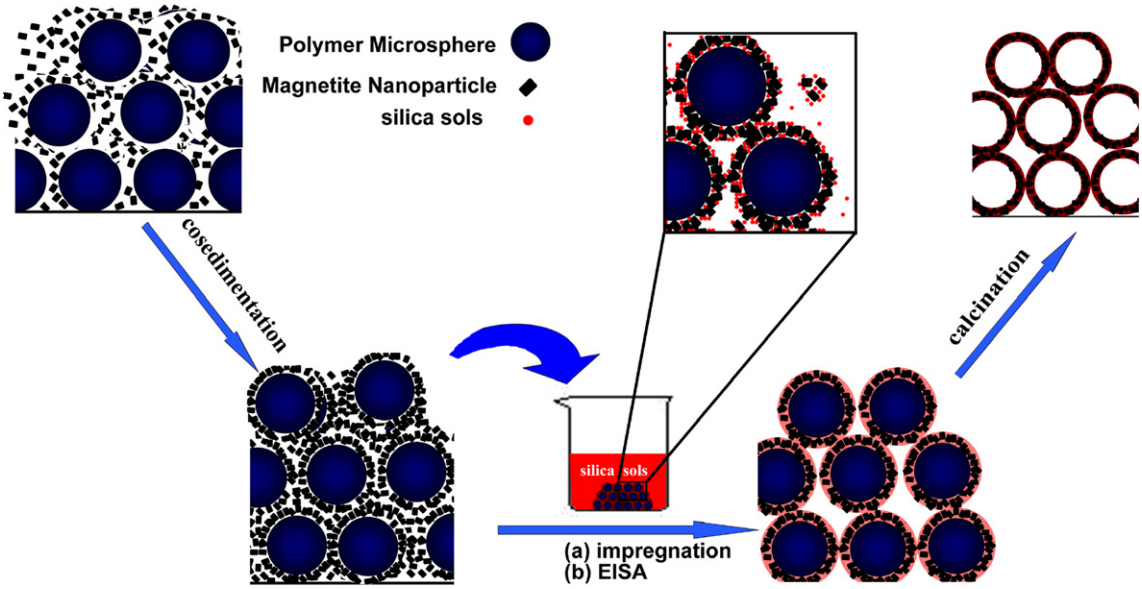

Scheme 1. The synthesis procedure to the magnetic/silica hybrid hollow microspheres.

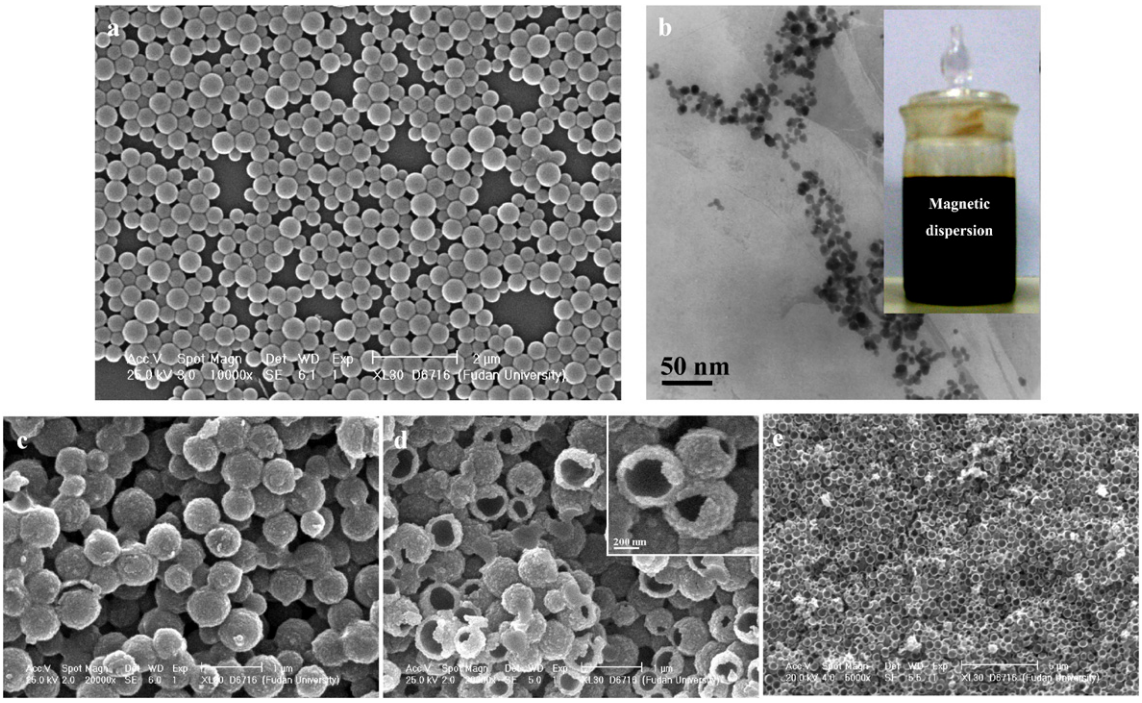

Fig. 1. SEM images of (a) the Poly(St-*co*-TMSPM) microspheres; TEM image of (b) Fe_3O_4 nanoparticles; SEM images of (c) the polymer/Fe_3O_4/silica composites obtained by cosedimentation of Fe_3O_4 nanoparticles and polymer microspheres with weight ratio of 1:1, (d) magnetic hollow Fe_3O_4/silica hybrid microspheres. The inset in (b) is the photograph of the aqueous dispersion containing magnetite nanoparticles (0.4 wt%). (e) SEM image of hollow magnetite/silica microspheres crushed to hemispheres, indicating that all the microspheres have typical hollow structure.

monomers. The microspheres used in this study have a mean diameter of 500 nm as determined from the SEM image (Fig. 1a). Because of the hydrophilic PVP attached on the surface of the polymer microspheres, they can be readily dispersed in water. Nanosized magnetite particles with diameter of less than 10 nm can be synthesized according to the reported method [36,37]. The TEM image shows that the particles have relatively uniform size and high dispersibility in water (Fig. 1b). The weight ratio of magnetite to the polymer microspheres is adjusted to 1:1. The homogeneous brown appearance of the polymer/Fe_3O_4 composite flakes suggests that the magnetite nanoparticles are uniformly distributed. After impregnation with silica, the polymer/Fe_3O_4/silica composite flakes show uniform brown-yellow appearance. SEM observation indicates that the flakes consist of microspheres with rough surface, suggesting the existence of the magnetite nanoparticles (Fig. 1c). The subsequent removal of the polymer microspheres yields hollow microspheres of about 400 nm in diameter (Figs. 1d and 1e), smaller than that of the polymer microspheres (500 nm). It reflects a large shrinkage of about 20% after pyrolysis due to the condensation of silica gels. The obtained sample powder was ground before measurement in order to observe the inner structure of hollow spheres. As measured from the broken hollow microspheres, the wall thickness is about 30 nm. The rough surface of the hollow microspheres reveals the presence of particles incorporated

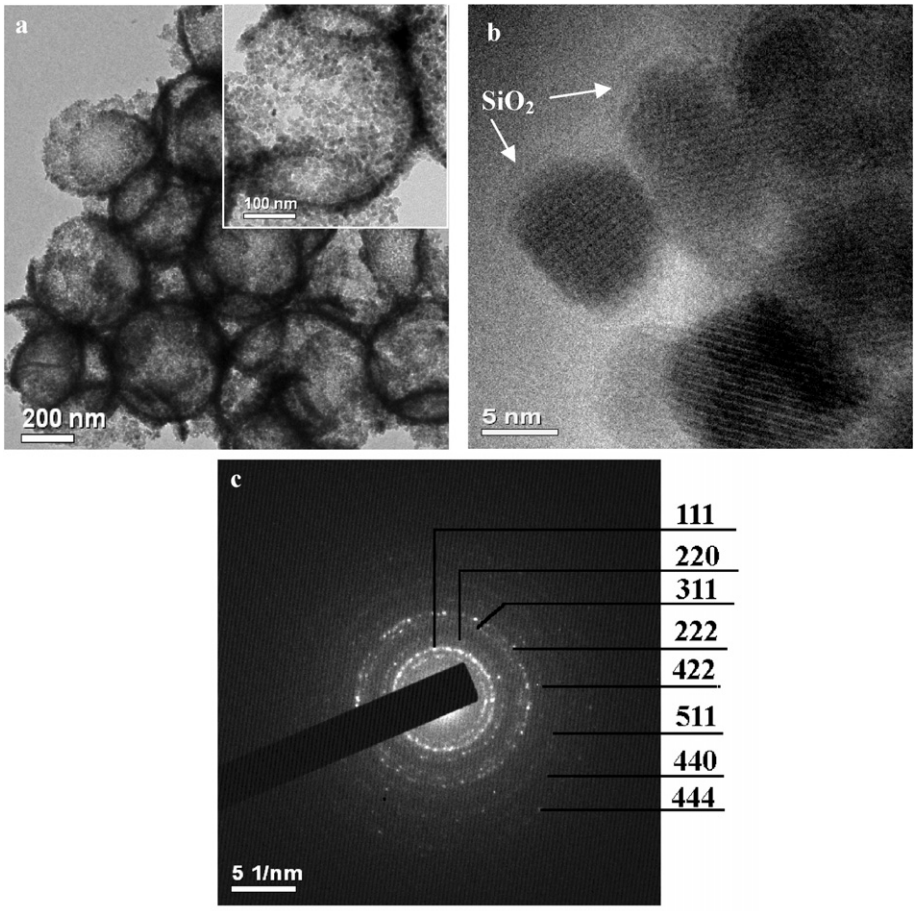

Fig. 2. TEM images (a, b) and the selective area electron diffraction pattern (c) of the magnetic hollow Fe_3O_4/silica hybrid microspheres.

in the walls. TEM image (Fig. 2a) reveals typical hollow structure of the microspheres with diameter of about 400 nm and rough walls consisting of numerous nanoparticles (Fig. 2a, inset). Many nanopores are observed in the walls of the hollow microspheres (Fig. 2a, inset), which are presumably generated by the intense shrinkage of the silica gels and the removal of polymer microspheres during the calcination. The porous walls may provide the hollow microspheres with high surface area and large amount of entryways for guests to access the macropores. Lattice fringes are observed for the pore walls of hollow microspheres in high resolution TEM (HRTEM) image (Fig. 2b), indicating that the magnetic nanoparticles with the size of about 5–10 nm are well-retained after the pyrolysis. Moreover, the amorphous species are also observed in the area around the nanocrystals, indicative of formation of silica around the magnetic nanoparticles. Selected area electron diffraction (SAED) pattern (Fig. 2c) recorded on the walls displays spotty diffraction rings, which can be assigned to the characteristic diffractions of magnetite. It reveals a polycrystalline feature of the magnetic hollow microspheres.

The XRD pattern of the magnetic hollow microspheres shows resolved diffractions similar to that of the magnetite nanoparticles, indicating that the magnetite structure is well retained during the process (Fig. 3). According to Debye–Scherer formula, calculations based on the strongest 311 diffraction peak reveal grain size of ~7.2 nm for the as-synthesized magnetite nanoparticles and 6.3 nm for the magnetite in the hollow microspheres. The slightly smaller grain size of the latter is probably due to the partial corrosion of the magnetite nanoparticles attached to microspheres during the impregnation with silicate oligomer solution containing small amount of HCl solution. The additional peak in

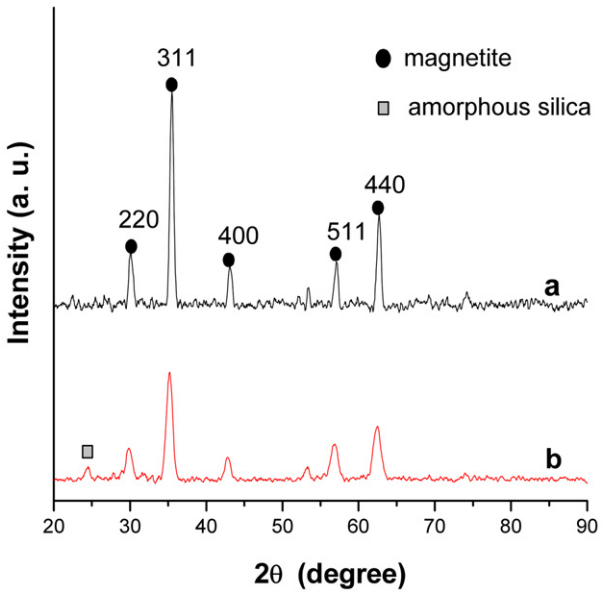

Fig. 3. XRD patterns of (a) magnetite nanoparticles and (b) magnetite/silica hybrid hollow microspheres obtained by cosedimentation of magnetite nanoparticles and polymer microspheres with weight ratio of 1:1.

the XRD pattern may be due to silica in the hollow sphere. Magnetic characterization at 300 K shows that the synthesized magnetite nanoparticles and hollow microspheres have magnetization saturation values of 32.3 and 23.1 emu/g, respectively (Fig. 4), both higher than that (13 emu/g) of magnetic microspheres reported

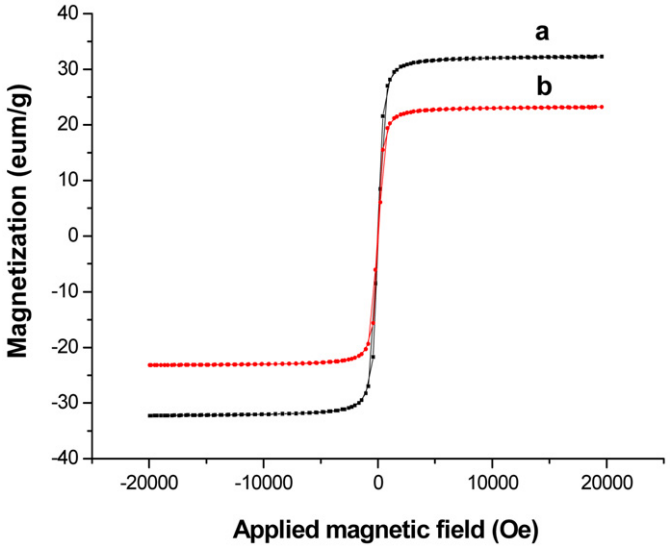

Fig. 4. The magnetic hysteresis loops of (a) magnetite nanoparticles and (b) magnetite/silica hybrid hollow microspheres recorded at 300 K. The magnetic hollow microspheres were obtained by cosedimentation of magnetite nanoparticles and polymer microspheres with weight ratio of 1:1.

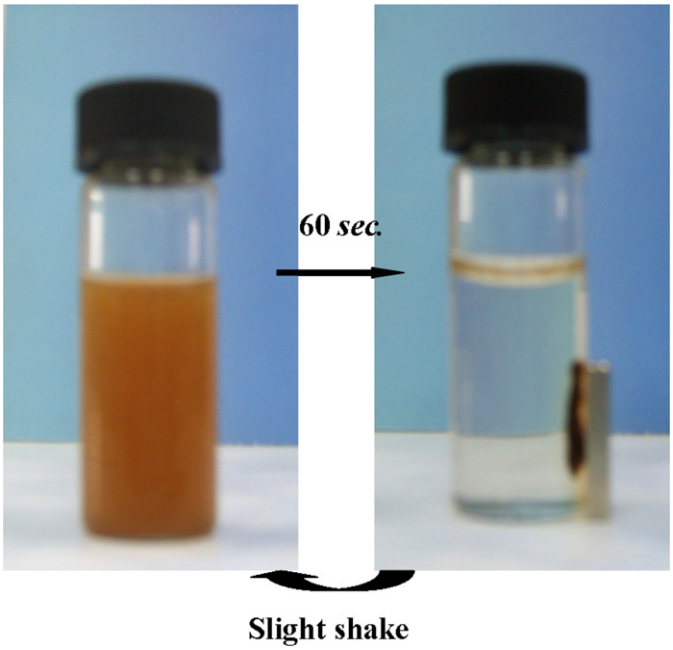

Fig. 5. Photographs for the separation and re-dispersion process of magnetite/silica hybrid hollow microspheres in aqueous dispersion.

by Tartaj et al. [38]. It reflects a high mass fraction (71.5 wt%) of magnetic component in the hybrid walls. The high magnetization may render the magnetic hollow microspheres rapid response to the applied external magnetic field, and thus ensuring a fast magnetic manipulation in practical applications. Additionally, no remanence was detected for both two samples, suggesting a superparamagnetic property. The hollow microspheres can be easily dispersed in aqueous solution simply by ultrasonication in a water bath, and they can be separated to the vessel wall in 60 s with a magnet of 1000 Oe (Fig. 5), and once the external magnetic field is removed, they can be re-dispersed quickly with a slight shake. The excellent magnetic properties and dispersibility of the hollow microspheres make them good candidates for various applications such as bioseparation, drug loading and catalyst carriers.

The TG analysis performed under N_2 atmosphere shows three-stage weight loss for the silica impregnated magnetite-adsorbed polymer microspheres (supporting information, Fig. S1). The small weight loss (9.0 wt%) in the range of 25–100 °C is due to the removal of physically adsorbed water and slight dehydration of silanol groups. A large weight loss of about 40 wt% is detected in the range of 350–500 °C with a sharp peak centered at 430 °C, which is predominantly attributed to the decomposition of polymer microspheres. The minor weight loss of about 4 wt% occurred at the higher temperature of 600–800 °C is due to the complete dehydration of silica species. Fourier transform infrared (FT-IR) spectra (Fig. S2) for silica-impregnated polymer microspheres/Fe_3O_4 shows absorption band at 2800–3100 cm^{-1} and the peaks at 1840–1940 cm^{-1} both associated with polystyrene, and typical band at 1090 cm^{-1} for the Si–O–Si vibration and peak at 570 cm^{-1} for the magnetite (Fig. S2a). After the pyrolysis, the obtained magnetic hollow microspheres show absorption bands of silica and magnetite at 1090 and 570 cm^{-1}, respectively, and the bands associated with organic species disappeared, suggesting the full decomposition of polymer microsphere templates (Fig. S2b). N_2 sorption isotherms of the magnetic hollow microspheres show irregular sorption–desorption curves (not shown). Calculation using BJH model shows a broad pore distribution in the range of 2 to 80 nm. It may be attributed to the holes on the surface made by accumulation of nanoparticles and some pores originated from the hollow sphere's packing, because the sample was not fully ground to prevent the hollow microspheres from being broken. The BET surface and pore volume are 67.6 m^2/g and 0.14 cm^3/g, respectively.

The formation of magnetic hollow microspheres is mainly attributed to two important factors. The first is the rapid packing process of polymer microspheres with attached magnetite nanoparticles during the fast solvent evaporation. Because the size of magnetite nanoparticles is far smaller than that of polymer microspheres, the nanoparticles precipitate spontaneously onto the microspheres to reduce surface energy during the cosedimentation, which leads to the packing of polymer microspheres with surfaces coated by numerous magnetite nanoparticles. The magnetite nanoparticle coating acts as the insulator for the neighboring polymer microspheres. The second is the formation of silica protection coating for the magnetite nanoparticles. During the impregnation treatment of polymer/Fe_3O_4 composite flakes with diluted silicate oligomer solution, the silicate species deposit on and encapsulate the magnetite-adsorbed polymer microspheres due to the strong affinity between the magnetite colloids and silica. In the process of pyrolysis, the inorganic silica coating further condenses on the microspheres' surface and the polymer microspheres are continuously decomposed, resulting in packing of hollow microspheres. The resultant packed hollow microspheres can be easily disassembled into single hollow microsphere after ultrasonication in water due to their weak interaction among the spheres.

It is worthy noting that the impregnation should be performed in a well-controlled way to ensure only small amount of silica be introduced, so that silica can coat the magnetite-adsorbed polymer microspheres. Otherwise, the confined interstitial voids in the polymer/Fe_3O_4 flakes would be fully filled with silica, and the obtained product is 3D macroporous materials, rather than hollow microspheres (Fig. S3). The magnetite nanoparticles play two key roles in the formation of hollow microspheres, i.e. isolating the polymer microspheres from each other and adsorbing small amount of silica species. It is worthy of noting that if the polymer microspheres were not separated by magnetite nanoparticles before impregnation, the obtained product could still be 3D macroporous material. The wall thickness of the hollow microspheres is mainly determined by the weight ratio of magnetite to the poly-

mer microspheres. When the weight ratio is 0.5, the wall thickness decreases to less than 20 nm, and the hollow microspheres with deformed morphology are obtained due to their poor mechanical stability (Fig. S4).

4. Conclusion

In summary, we have demonstrated a simple approach based on the co-sedimentation and impregnation to the fabrication of novel hollow microspheres with magnetite/silica hybrid walls. The obtained hollow microspheres have high magnetization of 23 emu/g and thus good magnetic responsivity. Additionally, disordered nanopores in the walls are readily observed. The void size of the hollow microspheres can be controllable from hundreds of nanometers to micrometers by using polymer microspheres with different sizes as templates, and the wall thickness can be adjusted from 10 to 50 nm by controlling the weight ratio of magnetite over the polymer microspheres. Due to the unique magnetic properties, large void size and permeable walls, the magnetic hollow microspheres possess high potential applications such as controlled drug delivery, biomacromolecule separation, and movable nanoreactor.

Acknowledgments

This work was supported by NSF of China (20721063, 20521140450, 20871030 and 20890120), State Key Basic Research Program of PRC (2006CB932302), Shanghai Leading Academic Discipline Project (B108), Doctoral Program Foundation of State Education Commission of China (200802461013) and the Shanghai Rising-Star Program (08QA14010).

Supporting information

Electronic supplementary information (ESI) available: TGA and DTG curves of TG curve and DTG curves of the silica-impregnated polymer/Fe_3O_4 composites, FT-IR spectra of silica-impregnated polymer/Fe_3O_4 composites before and after calcinations, SEM images of 3D macroporous magnetic silica structure, TEM and SEM images of magnetic hollow microspheres with thin wall.

Please visit DOI: 10.1016/j.jcis.2009.02.013.

References

[1] W. Meier, Chem. Soc. Rev. 29 (2000) 295.
[2] C.S. Peyratout, L. Dihne, Angew. Chem. Int. Ed. 43 (2004) 3762.
[3] F. Caruso, R.A. Caruso, H. Mohwald, Science 282 (1998) 111.
[4] Y.F. Zhu, J.L. Shi, W.H. Shen, X.P. Dong, J.W. Feng, M.L. Ruan, Y.S. Li, Angew. Chem. Int. Ed. 44 (2005) 5083.
[5] D. Walsh, B. Lebeau, S. Mann, Adv. Mater. 11 (1999) 324.
[6] S.H. Im, U. Jeong, Y.N. Xia, Nat. Mater. 4 (2005) 671.
[7] M. Yang, J. Ma, C.L. Zhang, Z.Z. Yang, Y.F. Lu, Angew. Chem. Int. Ed. 44 (2005) 6727.
[8] H.P. Liang, H.M. Zhang, J.S. Hu, Y.G. Guo, L.J. Wan, C.L. Bai, Angew. Chem. Int. Ed. 43 (2004) 1540.
[9] Q. Liu, H.J. Liu, M. Han, J.M. Zhu, Y.Y. Liang, Z. Xu, Y. Song, Adv. Mater. 17 (2005) 1995.
[10] X.W. Lou, C. Yuan, Q. Zhang, L.A. Archer, Angew. Chem. Int. Ed. 45 (2006) 3825.
[11] H.G. Wang, X.M. Zheng, C. Ping, X.M. Zheng, J. Mater. Chem. 16 (2006) 4701.
[12] Q. Peng, Y.J. Dong, Y.D. Li, Angew. Chem. Int. Ed. 42 (2003) 3027.
[13] Y.J. Xiong, B.J. Wiley, J.Y. Chen, Z.Y. Li, Y.D. Yin, Y.N. Xia, Angew. Chem. Int. Ed. 44 (2005) 7913.
[14] H.G. Yang, H.C. Zeng, Angew. Chem. Int. Ed. 43 (2004) 6056.
[15] A. Antipov, G. Sukhorukov, Y. Fedutik, J. Hartmann, M. Giersig, H. Möhwald, Langmuir 18 (2002) 6687.
[16] C.I. Zoldesi, A. Imhof, Adv. Mater. 17 (2005) 924.
[17] X.L. Xu, S.A. Asher, J. Am. Chem. Soc. 126 (2004) 7940.
[18] Y.G. Sun, Y.N. Xia, Science 298 (2002) 2176.
[19] A.M. Cao, J.S. Hu, H.P. Liang, L.J. Wan, Angew. Chem. Int. Ed. 44 (2005) 4391.
[20] J.H. Gao, B. Zhang, X.X. Zhang, B. Xu, Angew. Chem. Int. Ed. 45 (2006) 1220.
[21] G.W. Nyce, J.R. Hayes, A.V. Hamza, J.H. Satcher, Chem. Mater. 19 (2007) 344.
[22] Z.Y. Zhong, Y.D. Yin, B. Gates, Y.N. Xia, Adv. Mater. 12 (2000) 206.
[23] S.W. Kim, M. Kim, W.Y. Lee, T. Hyeon, J. Am. Chem. Soc. 124 (2002) 7642.
[24] H. Cölfen, Macromol. Rapid Commun. 22 (2001) 219.
[25] X.W. Lou, Y. Wang, C.L. Yuan, J.Y. Lee, L.A. Archer, Adv. Mater. 18 (2006) 2325.
[26] S. Biggs, K. Sakai, T. Addison, A. Schmid, S.P. Armes, M. Vamvakaki, V. Bütün, G. Webber, Adv. Mater. 19 (2007) 247.
[27] D. Gorin, D. Shchukin, A. Mikhailov, K. Köhler, S. Sergeev, S. Portnov, I. Taranov, V. Kislov, G. Sukhorukov, Tech. Phys. Lett. 32 (2006) 70.
[28] D. Shchukin, D. Gorin, M. Helmuth, Langmuir 22 (2006) 7400.
[29] A. Antipov, G. Sukhorukov, Y. Fedutik, J. Hartmann, M. Giersig, H. Möhwald, Langmuir 18 (2002) 6687.
[30] Z.H. Dai, J. Zhang, J.C. Bao, X.H. Huang, X.Y. Mo, J. Mater. Chem. 17 (2007) 1087.
[31] D. Radziuk, D.G. Shchukin, A. Skirtach, H. Mohwald, G. Sukhorukov, Langmuir 23 (2007) 4612.
[32] F. Caruso, M. Spasova, A. Susha, M. Giersig, R.A. Caruso, Chem. Mater. 13 (2001) 109.
[33] F. Caruso, Adv. Mater. 13 (2001) 11.
[34] R. Qiao, X.L. Zhang, R. Qiu, J.C. Kim, Y.S. Kang, Chem. Mater. 19 (2007) 6485.
[35] Y.H. Deng, C. Liu, J. Liu, F. Zhang, T. Yu, F.Q. Zhang, D. Gu, D.Y. Zhao, J. Mater. Chem. 18 (2008) 408.
[36] I. Nedkov, T. Merodiiska, L. Milenova, T. Koutzarova, J. Magn. Magn. Mater. 21 (2000) 296.
[37] Y.H. Deng, W.L. Yang, C.C. Wang, S.K. Fu, Adv. Mater. 15 (2003) 1729.
[38] P. Tartaj, T.G. Carreæo, C.J. Serna, Adv. Mater. 13 (2001) 1620.